

# Structural, Optical and Gas Sensing Properties of TiO<sub>2</sub>-MoO<sub>3</sub> Thin Films

P. V. Kala<sup>1</sup>, B. T. Rao<sup>2</sup> and K. Srinivasarao<sup>3\*</sup>

<sup>1</sup> Department of Basic Sciences & Humanities, Vignan's Lara Institute of Technology & Science, Vadlamudi – 522 213.

<sup>2</sup> Laser Division, Raja Ramanna Centre for Advanced Technology, Indore – 452 013.

<sup>3</sup> Department of Applied Sciences & Humanities, Sasi Institute of Technology & Engineering, Tadepalligudem – 534 101, Andhra Pradesh, India.

Received: 3 Mar. 2019, Revised: 3 Jun. 2019, Accepted: 17 Jul. 2019

Published online: 1 Sep. 2019

**Abstract:** Thin films of TiO<sub>2</sub> - MoO<sub>3</sub> were deposited on quartz glass, Silicon (100) substrates by dc magnetron sputtering at two substrate temperatures of 300 K and 600 K and at a fixed sputtering pressure of 5 Pa and sputtering power of 50 W respectively. The atomic percent of (at.%) titanium (Ti) in composite is found to be 1 and 2.4. The deposited films were characterized by X-ray Photo Electron Spectroscopy (XPS) and Optical Transmittance studies. The optical transmittance of the MoO<sub>3</sub> films deposited at 300 K, 5 Pa is 60 % and increases with increasing Ti at.%. The energy gap of the films is 3.7 eV and increases with increasing Ti at. %. The optical transmittance is further increasing when the films were deposited at 600 K, reaching 98 % and decreases with increasing Ti at. %. The energy gap of the film is 3.94 eV and decreases with increasing Ti at. %. The composite films showed good sensitivity and fast response time when exposed to CO.

**Keywords:** TiO<sub>2</sub>-MoO<sub>3</sub> thin films, XPS, XRD, optical transmittance, gas sensing property.

## 1 Introduction

Among oxides transition metals oxides are found to be promising candidates which finds many applications in the field of science and technology. Among various applications, the devices like gas sensors [1,2], electrochromic [3,4], photochromic [5], and thermochromic [6], samples, made up by using these materials occupy, an important place among materials. Moreover the physical properties like optical transmittance, resistivity and energy gap can be tuned to required value by forming these materials as composites. The purpose of forming a composite is not only to tune a physical property but also to improve it. Several composites like MoO<sub>3</sub>-WO<sub>3</sub> [7] MoO<sub>3</sub>-V<sub>2</sub>O<sub>5</sub> [8], WO<sub>3</sub>-V<sub>2</sub>O<sub>5</sub> [9] and, TiO<sub>2</sub>-MoO<sub>3</sub> [10, 11] were formed by researchers and experimentally demonstrated that tune and improve in the various physical properties like electrochromism, photochromism and gas sensitivity and water treatment [12]. Among the above

composites the MoO<sub>3</sub>-WO<sub>3</sub> does not show any increment in the conductivity and stability at high temperatures i.e. above 700 K. Similarly the formation of MoO<sub>3</sub>-V<sub>2</sub>O<sub>5</sub> composite film is difficult and it is quite unstable in the film form. Similarly, lines WO<sub>3</sub>-V<sub>2</sub>O<sub>5</sub> has found applications in different fields like bolometers etc. The TiO<sub>2</sub>-MoO<sub>3</sub> composite is found [10,11] to be a promising candidate in terms of the formation of a stable compound, and of improving in electrical conductivity and maintenance of the composite state at high temperatures. The composite which is used as a gas sensor should exhibit good sensitivity and fast response when exposed to different gases. This can be achieved, in the case of TiO<sub>2</sub>-MoO<sub>3</sub> by the addition of TiO<sub>2</sub> to MoO<sub>3</sub>. So it is possible to tune the optical properties like transmittance, energy gap and electrical resistivity in TiO<sub>2</sub>-MoO<sub>3</sub> composite such that it would exhibit good sensitivity and fast response when exposed to different gases [13,14]. In the present investigation thin films of TiO<sub>2</sub>-MoO<sub>3</sub> composite were prepared by changing the TiO<sub>2</sub> content and their substrate

\*Corresponding author: [kotaririnu@yahoo.co.in](mailto:kotaririnu@yahoo.co.in)

temperatures during the deposition process.

## 2 Experimental Technique

Dc magnetron sputtering was used to deposit thin films of TiO<sub>2</sub>-MoO<sub>3</sub> in a vacuum coating unit supplied by VR Technologies, Bangalore, India. The vacuum chamber is initially thoroughly cleaned with acetone to prevent any degassing then it was evacuated to a pressure of 10<sup>-6</sup> mbar (measured by using a digital penning gauge which is calibrated with a Baured Alpert gauge) by using a diffusion pump backed by a rotary pump. A high purity Mo and Ti mosaic target of 3 mm thickness and 2.54 cm diameter was used to prepare thin films at various sputtering pressures and temperatures. The sputtering process was initiated by flowing Ar gas first and then oxygen was flown in to the vacuum chamber. The target was presputtered for few minutes and the flow rate both gases was controlled by a needle valve. The substrates were precleaned before fixing them to the substrate holder and their ion bombardement was also performed before deposition. The sputtering power during the deposition was maintained at 50 W. The X-ray photo electron spectrum was recorded by using a PHI 5000 Versa Probe II, FEI Inc. The XPS spectrum was recorded performed in the scanning energy range of 0 – 1200 eV. The spectral resolution was 1 eV. The XRD spectrum was recorded for the films deposited on Si (100) substrates at a glancing angle of 0.5° in order to determine their structure by using a Panalytical X ray diffractometer. The surface microstructure was studied by using FESEM microscopy (Zeiss, Model : Sigma 300). The optical transmittance spectra of the films was recorded in the 300 – 1100 nm wavelength range by using an UV-VIS spectrophotometer. The resolution of the instrument is 4 nm. The thickness of the films is 3000 Å which was measured by means of a stylus profilometer (Veeco DEKTAK 150). The thickness resolution of the instrument is ±10Å.

## 3 Results and Discussion

### 3.1 XPS Studies

The X-ray photo electron spectra of MoO<sub>3</sub> and TiO<sub>2</sub>-MoO<sub>3</sub> thin films were recorded to know their composition and chemical state. The XPS survey spectrum of MoO<sub>3</sub> thin films deposited at 5 Pa and 300 K is shown in Fig.1. The XPS spectrum was calibrated by the C 1s peak (284.6 eV). The high resolution analyses of the O 1s and Mo 2p peaks are shown in Fig. 4. The characteristic peaks of Mo are observed at 231 eV and 234.22 eV and are due to Mo 3d<sup>5/2</sup> and 3d<sup>3/2</sup> while oxygen peak is at 529 eV and it is due to O 1s in the case of undoped MoO<sub>3</sub> thin films. This indicates the Mo<sup>6+</sup> state of Mo in MoO<sub>3</sub>. The atomic percent of individual elements was estimated by using the deconvolution technique. The at.% of Mo is 25.18 and Oxygen is 74.82 %. The observed at.% of oxygen indicates

that there is a small at. % percent (0.18) of oxygen deficiency. This indicates the films were somewhat sub-stoichiometric.

The XPS spectrum (Fig. 2) of TiO<sub>2</sub>-MoO<sub>3</sub> films deposited at 5 Pa and 300 K shows the existence of Mo, O and Ti. The at. % percentage of Ti is 1 and Mo and oxygen were 23.41 and 75.59 respectively. There is a shift in the characteristic Mo peak position towards higher energy due to Titanium doping (see Fig.4). The characteristic peaks of Ti are observed at 460 eV and 464 eV and are due to the 2p<sup>3/2</sup> and 2p<sup>1/2</sup> states. This indicates the Ti<sup>4+</sup> state in TiO<sub>2</sub>. The XPS spectrum of films deposited at 600 K is shown in Fig. 3. The at. % of Ti is 2.4, Mo is 22.77 % and oxygen is 74.84 %. The at.% ratio of Oxygen to Mo is 3.12. The excess oxygen 0.12 at.% is corresponding to the oxygen in TiO<sub>2</sub>. The characteristic Ti peaks were observed at 453 eV and 460 eV. This indicates the characteristic shift in the 2p<sup>3/2</sup> and 2p<sup>1/2</sup> peaks towards lower energy. The shift in the peak position in case of Mo and Oxygen is towards lower energy. This may be due to the decrease of the energy required to extract an electron from Ti with decreasing Mo at. % in the composite. [15]. The oxygen 1s core level spectrum is shown in Fig. 5. It is observed that there is a shift in the 1s peak position with Ti at. %. But this shift is towards higher energy when Ti at.% is low and it is towards lower energy with increasing Ti at.%. The reason may be due to the amorphous (in case of Ti at.% = 1, Ts = 300 K) and polycrystalline phases (in case of Ti at. % = 2.4, Ts = 600 K) of the TiO<sub>2</sub>-MoO<sub>3</sub> composite.

### 3.2 X-ray Diffraction Studies

The X-ray diffraction spectra of TiO<sub>2</sub>:MoO<sub>3</sub> thin films deposited at 5 Pa and 300 K are shown in Fig. 7.

The undoped MoO<sub>3</sub> films crystallizes in orthorhombic phase (040) and crystallizes in mixed phases for 1 at. % of Titanium while for 2.4 at. % of Ti, they exhibit strong crystalline monoclinic phase [6,15]. The inter planar spacing is evaluated using the Bragg's law

$$n\lambda = 2d\sin\Theta \quad (1)$$

where n is the diffraction order,  
λ is the wavelength of X-rays in Å,  
d is the interplanar spacing, and  
Θ is the angle of diffraction in degrees.

In the present case the 2Θ value of the observed (040) orientation is 25.44. the 2Θ angle is shifting towards lower value with increasing Ti doping into MoO<sub>3</sub>. The observed shift is due to the films compression stress. The calculated d value is 3.498 Å. The lattice parameters a, b, c of undoped MoO<sub>3</sub> were calculated by using the following relation,

$$d_{hkl} = \frac{1}{\left[ \frac{h^2}{a^2} + \frac{k^2}{b^2} + \frac{l^2}{c^2} \right]^{1/2}} \quad (2)$$

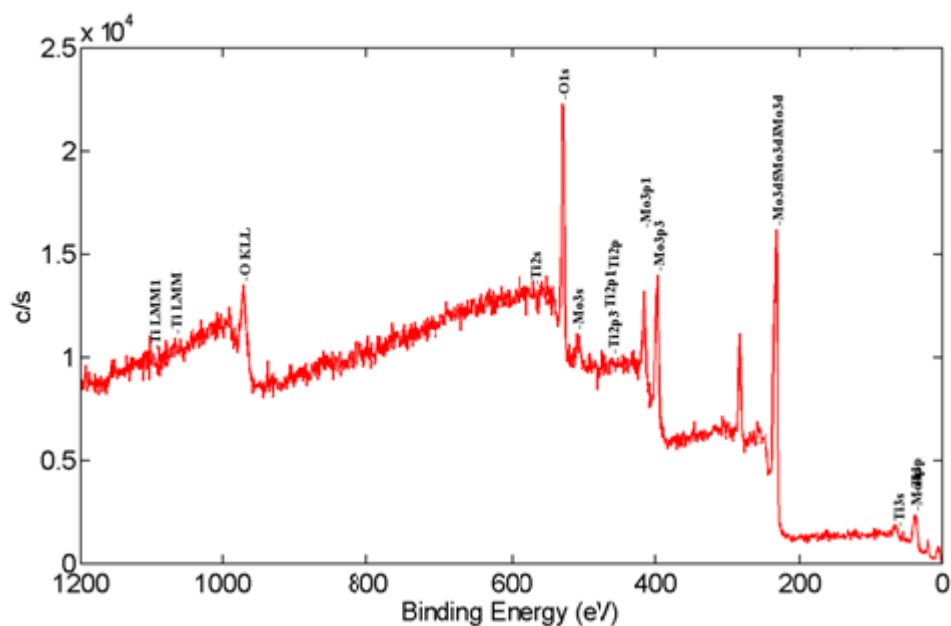


**Fig. 1:** XPS survey spectrum of MoO<sub>3</sub> thin films deposited at 600 K and sputtering pressure of 5 Pa. The at. % of Mo is 25.18 and Oxygen is 74.82.

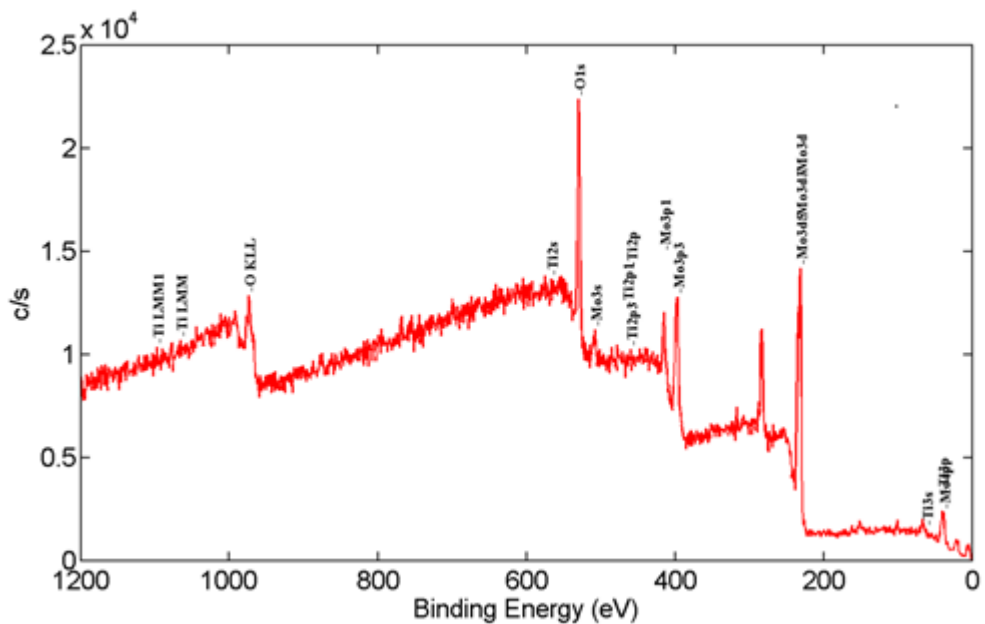


**Fig.2:** XPS survey spectrum of (TiO<sub>2</sub>)-MoO<sub>3</sub> thin films deposited at 300 K and sputtering pressure of 5 Pa. The at. % of Titanium is 1, Mo is 23.41 and Oxygen 75.59.

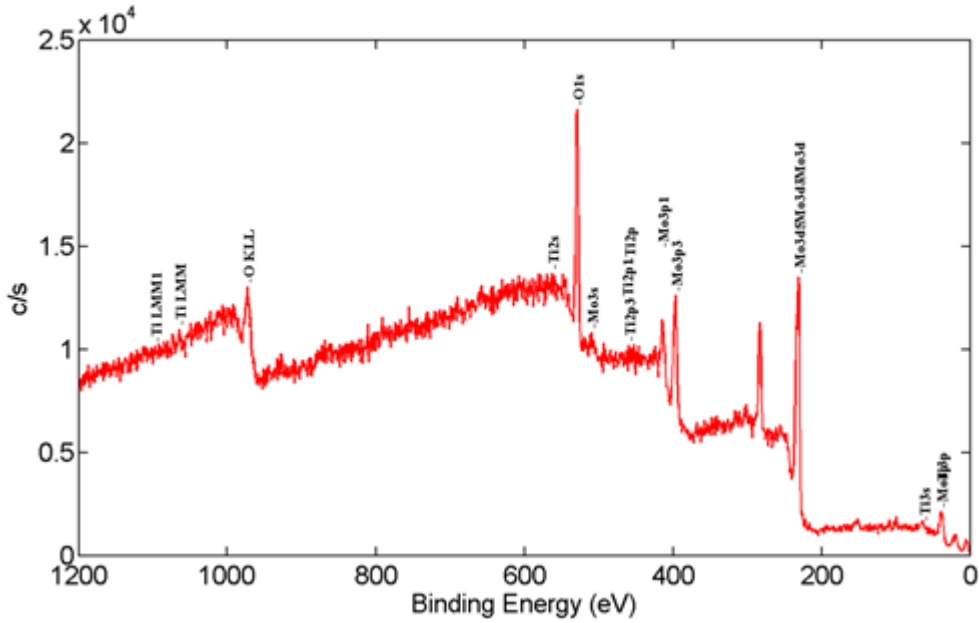


**Fig. 3:**XPS survey spectrum of (TiO<sub>2</sub>)-MoO<sub>3</sub> thin films deposited at 600 K and sputtering pressure of 5 Pa. The at. % of Titanium is 2.4, Mo is 22.77 and Oxygen 74.84.

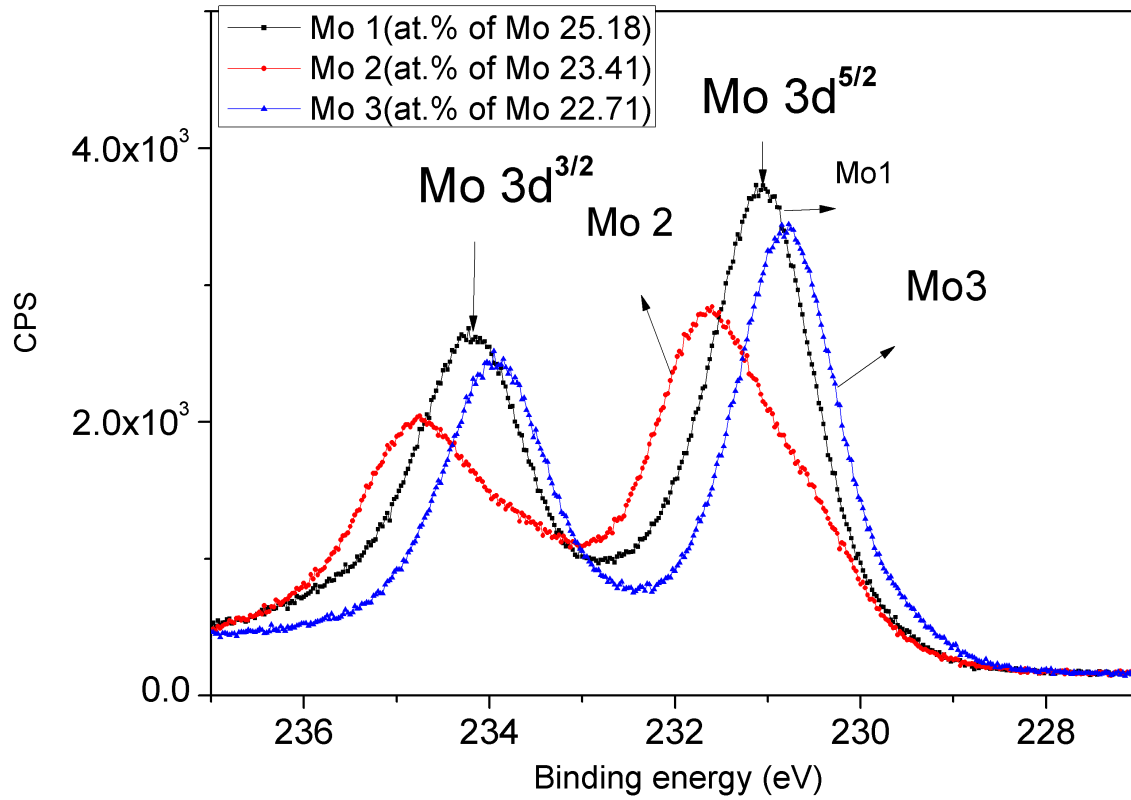


**Fig.4:** Variation of Binding energy of Molybdenum in MoO<sub>3</sub> and TiO<sub>2</sub> - MoO<sub>3</sub> thin films.

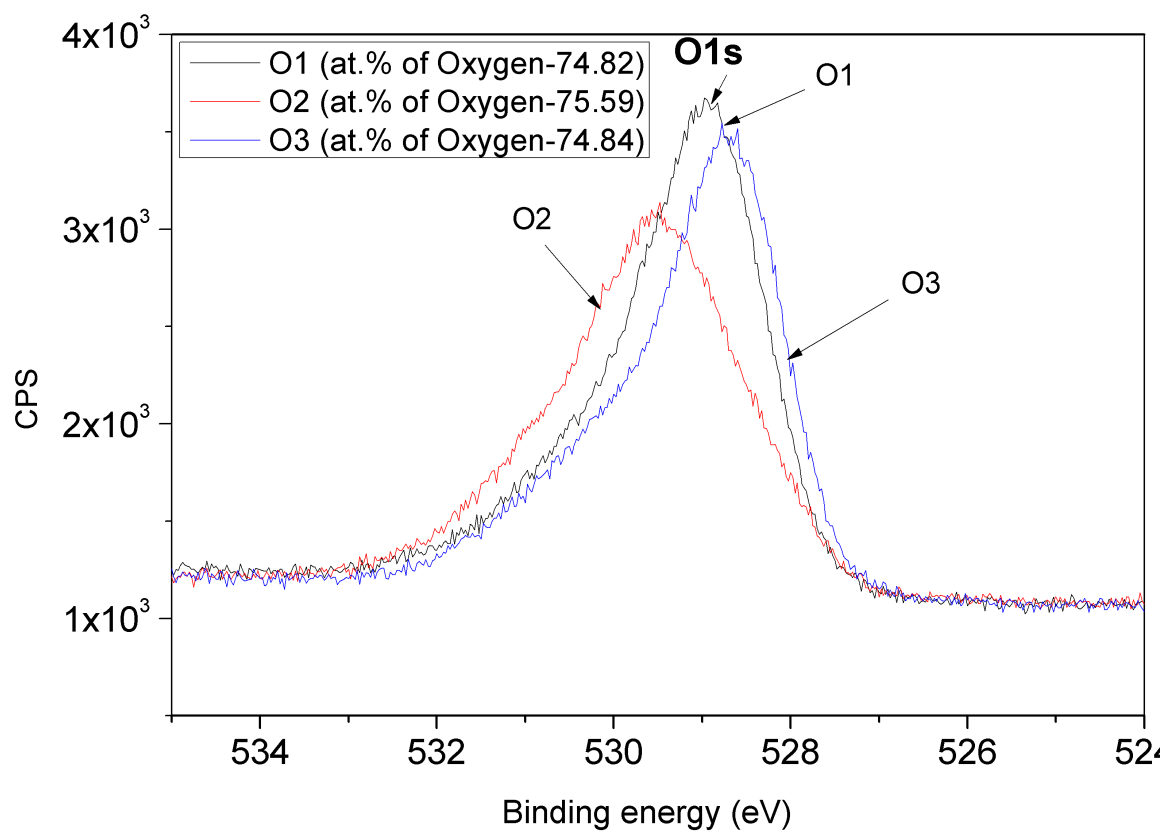


**Fig. 5:** Variation of Binding energy of Oxygen in  $\text{MoO}_3$  and  $\text{TiO}_2 - \text{MoO}_3$  thin films.

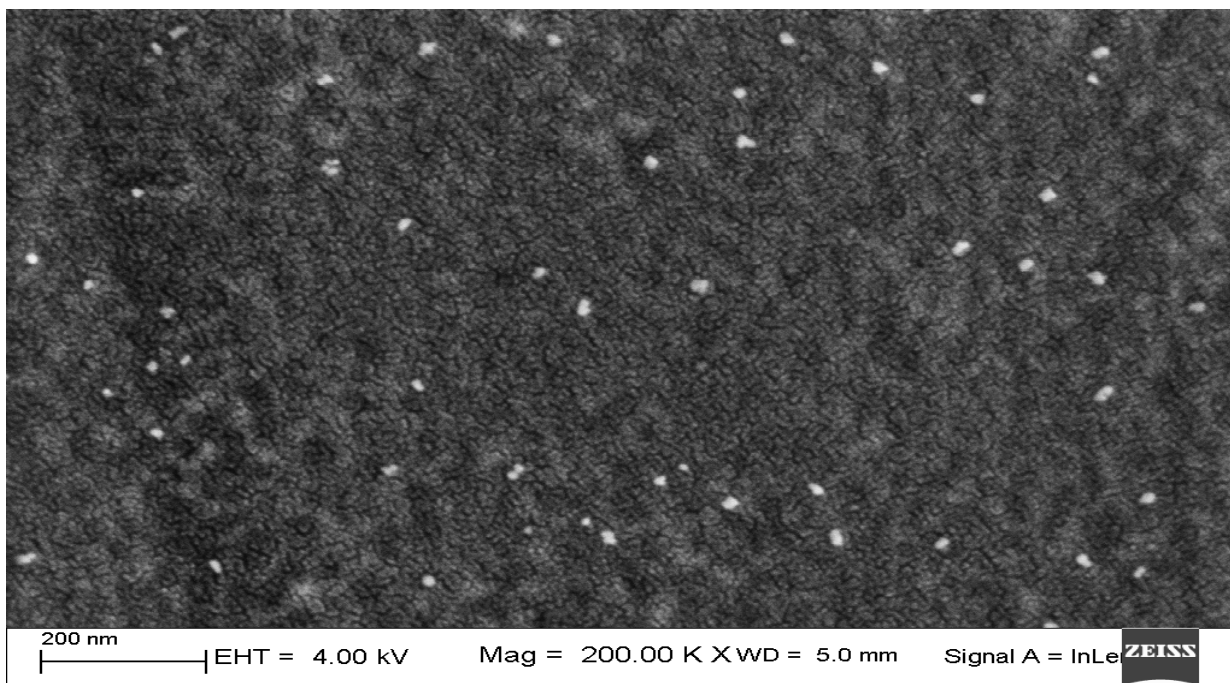


**Fig. 6:** FESEM image of  $\text{Ti:MoO}_3$  thin films deposited at 5 Pa and 300 K (Ti at. % is 1).

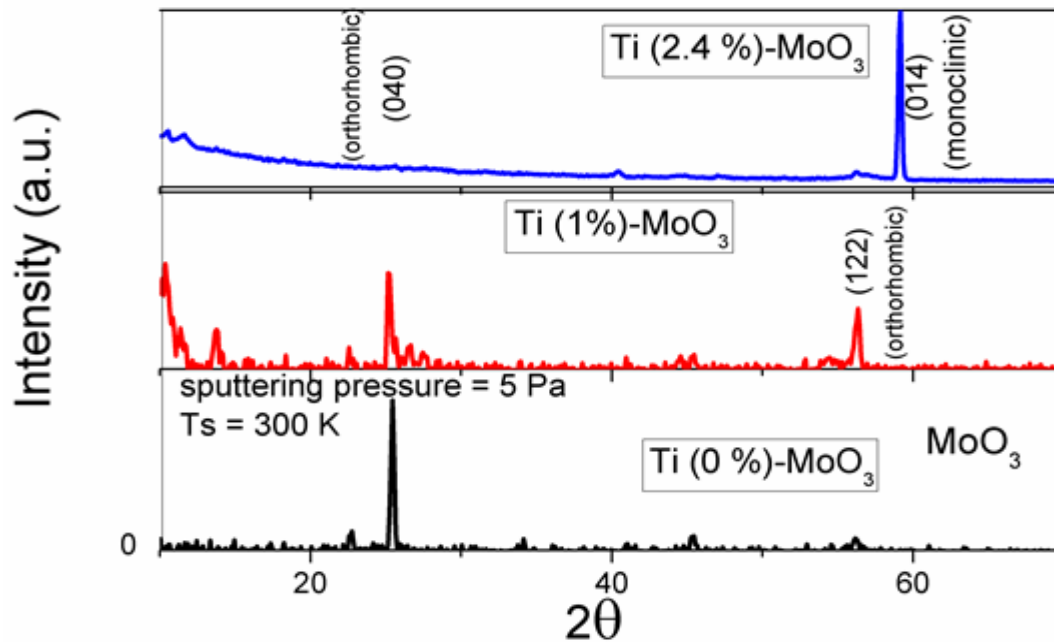


**Fig.7:** XRD of Ti:MoO<sub>3</sub> thin films deposited substrate temperature of 300 K and sputtering pressure of 5 Pa.

For (040) orientation, the obtained  $b$  value is 13.99 Å. The  $b$  value is increasing to 14.05 Å with increasing Ti at.% to 1. The other two parameters  $a$ ,  $c$  were evaluated by using the (120) and (021) crystallographic orientation, since we got only one peak corresponding to (040). The above crystallographic orientations are of the orthorhombic phase and are having the nearly same interplanar spacing as the one obtained in case of the (040) orientation. The evaluated  $a$ ,  $c$  values are 4.05 Å, 14.05 Å which are higher when compared to the single crystal MoO<sub>3</sub> [16] [JCPDS File no. 00-001-0615]. With increasing Ti at. % to 2.4 the films crystallizes in monoclinic phase with (014) (see also Fig. 7) orientation. The observed  $2\theta$  peak is at  $59.13^\circ$  (degrees). The  $d$  value obtained is 1.56 Å, which is very close the single crystalline MoO<sub>3</sub> [6] (JCPDS file num. 00-001-0615). So, the  $a$ ,  $b$ ,  $c$  values are 3.95 Å, 3.69 Å & 7.10 Å respectively. The grain size is estimated from Sherrer's law,

$$L = k\lambda/\beta\cos\Theta(3)$$

$L$  is the grain size,

$k$  is correction factor which is equal to 1.

$\beta$  is the full width at half maximum (in radians),

$\Theta$  is angle in degrees.

The calculated grain size is 31 nm.

The X-ray diffraction spectra of undoped MoO<sub>3</sub> and TiO<sub>2</sub>-MoO<sub>3</sub> composite deposited at a sputtering pressure of 5 Pa and substrate temperature of 600 K are shown in Fig. 8.

With increasing substrate temperature to 600 K the

undoped MoO<sub>3</sub> exhibited the crystallographic orientations (040) and (218) which correspond to the orthorhombic and hexagonal phases respectively [16]. The evaluated  $d_{040}$  is 3.51 Å which is an increment when compared to the films deposited at 300 K. The evaluated lattice parameter  $b$  is 14.03 Å which implies its small increase. With increasing Ti at. % to 1 at.% the films crystallizes again in the orthorhombic (040) phase with an increment in the interplanar spacing at 3.52 Å. The evaluated  $b$  value is 14.08 Å which is also indicates the increment as compared to the undoped MoO<sub>3</sub> films.

With further increasing Ti at. % to 2.4 the films crystallizes in monoclinic phase. The  $2\theta$  value is 59.20 degrees and corresponds to the (014) crystallographic orientation. The evaluated  $d$  value is 1.559 Å. The evaluated  $b$ ,  $c$  values are 3.49 Å and 6.97 Å respectively, which are low as compared to the ones for the films deposited at 300 K. The overall study indicates the films were in a compressive stress, when deposited at 300 K and the stress is increasing with Ti at. % and deposition temperature. Instead, the films crystallized in monoclinic phase are in tensile stress and the stress is increasing with substrate temperature [16-18].

### 3.3 Microstructural Studies

The microstructure of Ti:MoO<sub>3</sub> thin films deposited at 5 Pa and 300 K is shown in Fig. 9. The morphology reveals that the films contains micro particles of uniform size. The crystallite size is around 30 nm. This type of observed flat

morphologies proves to be more sensitive when exposed to different gases and shows significant change in resistivity with gas exposure [19-21].

### 3.4 Optical Transmittance

The optical transmittance spectra of the films was studied to know the optical quality and type of optical transition of the films. The optical transmittance of the MoO<sub>3</sub> films deposited at 300 K and 5 Pa is shown in Fig. 9. The transmittance of the films is 60 % and increases with increasing Ti at. %. The reason for this enhancement is due to the enhancement in the reactivity between Ti, Mo and oxygen.

The energy gap of the films was estimated by the formula, [22]

$$(\alpha h\nu) = B (h\nu - E_g)^{1/n} \quad (4)$$

where exponent 'n' takes the values 2 and 1/2 based on the type of electronic transition. In the present investigation the films showed better fit for n = 2 which indicates that the electron transition is direct. The energy gap is found by extrapolating the graph of  $(\alpha h\nu)^2$  versus  $h\nu$  (Fig. 10). The estimated energy gap of the pure MoO<sub>3</sub> films is 3.7 eV and increase with increasing Ti at. % [23]. The optical transmittance of the films deposited at 600 K and 5 Pa is shown in Fig. 11. The transmittance of the films is uptill 98 % and decrease with increasing Ti at.%. The reason for this decrease is given by more electron scattering and ionized impurity scattering at a higher carrier concentration, besides decrease in the solubility limit of Ti in MoO<sub>6</sub> matrix which leads to an increase of lattice

distortion in some regions [24]. The energy gap of the pure MoO<sub>3</sub> film is 3.94 eV and decreases with increasing Ti at. %. This may be due to an improvement in the crystallinity of the composite films which decreases the energy gap between conduction bands of TiO<sub>2</sub> and MoO<sub>3</sub> [25].

### 3.5 Gas Sensing Studies

TiO<sub>2</sub>:MoO<sub>3</sub> thin films were deposited on quartz substrates (10 mm x 5 mm) to study their gas sensing properties. Silver was evaporated in order to obtain the contacts to test the samples for gas sensitivity [26]. The contacts were found to be ohmic for a wide range of voltages. The testing of samples for different gases were performed by placing them on a sample holder inside the stainless steel chamber. A needle valve was used to maintain a constant flow rate 50 sccm of testing gas. A Keithly multimeter was used to measure the resistance of the sample.

The samples were exposed to CO gas and showed good sensitivity (see Fig. 13), .

The Sensitivity calculated by using

$$s = \frac{R_a - R_g \times 1}{R_a [\text{gas}]} \quad (5)$$

where  $R_a$  is the resistance of the film in air,  $R_g$  is the resistance of the test gas and  $[\text{gas}]$  is the concentration of the test gas.

It was found that the CO sensitivity was increasing with increasing Ti at. % in the TiO<sub>2</sub>-MoO<sub>3</sub> composite. The sensitivity of the films is maximum for Ti at. % of 2.4 . The results were in good agreement with reported values [1, 14,15, 27, 28]. The sensitivity of TiO<sub>2</sub>-MoO<sub>3</sub> thin films for different concentration of CO is shown in Fig. 13.

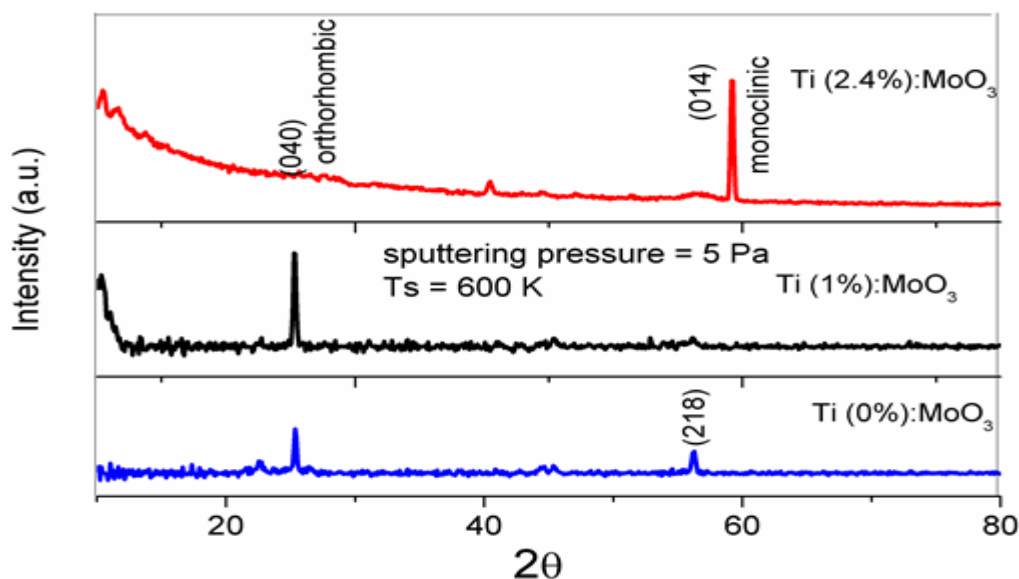


**Fig.8:** XRD of Ti:MoO<sub>3</sub> thin films deposited substrate temperature of 600 K and sputtering pressure of 5 Pa.

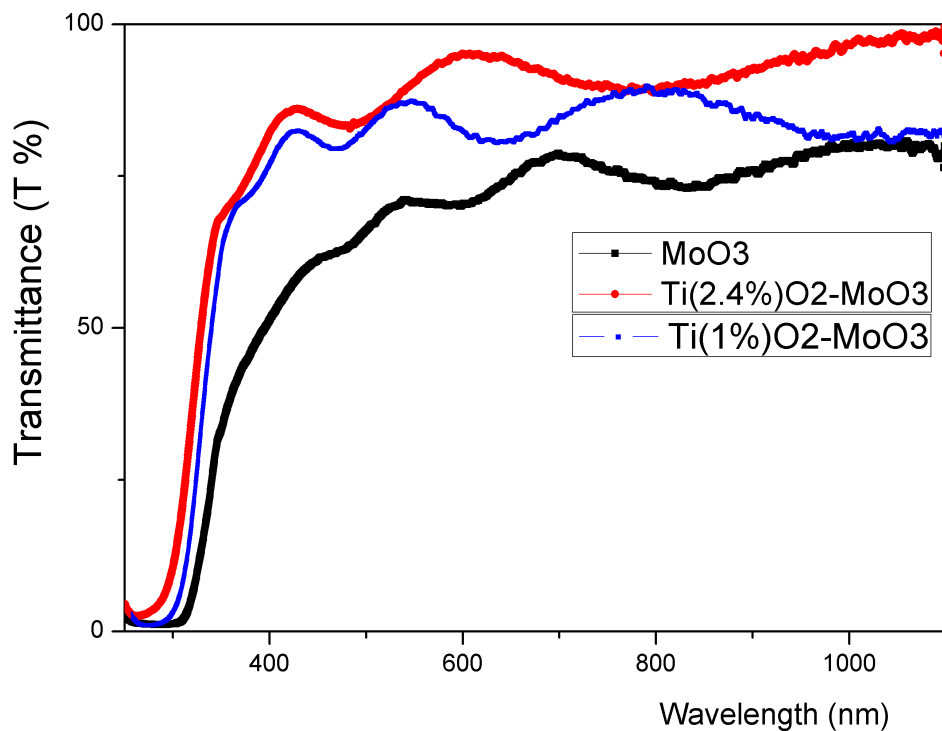


**Fig .9:** Optical transmittance spectra of MoO<sub>3</sub> and TiO<sub>2</sub>-MoO<sub>3</sub> thin films deposited at a sputtering pressure of 5 Pa and substrate temperature of 300 K.

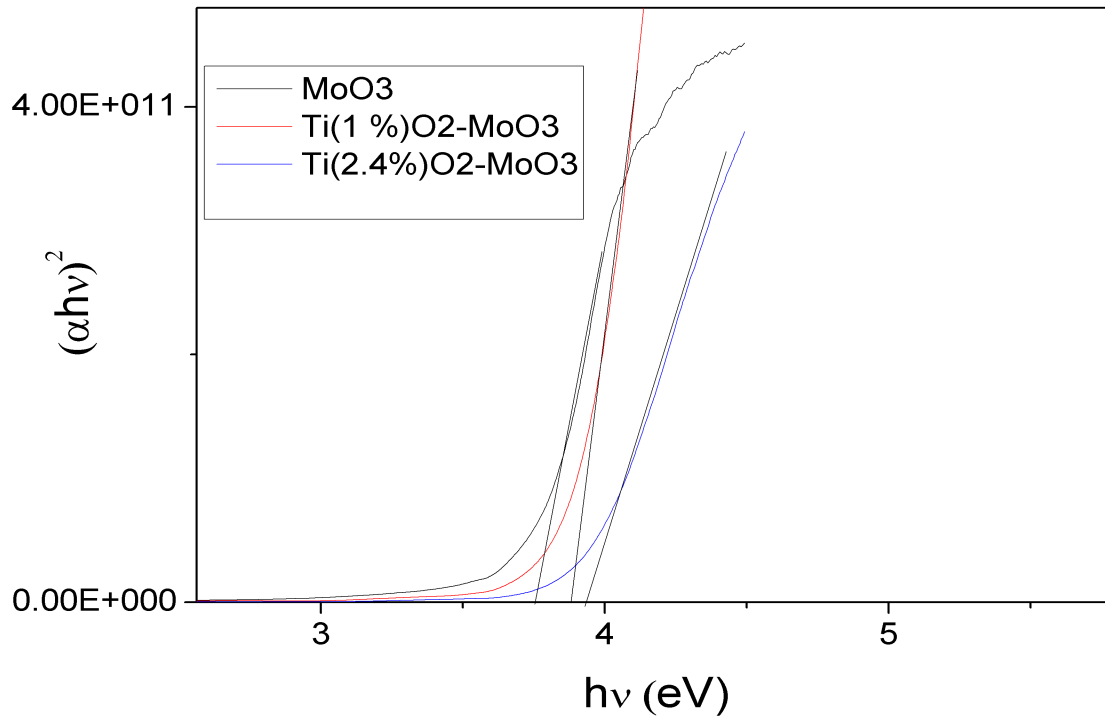


**Fig. 10:** Plots of  $(\alpha h\nu)^2$  vs  $h\nu$ .



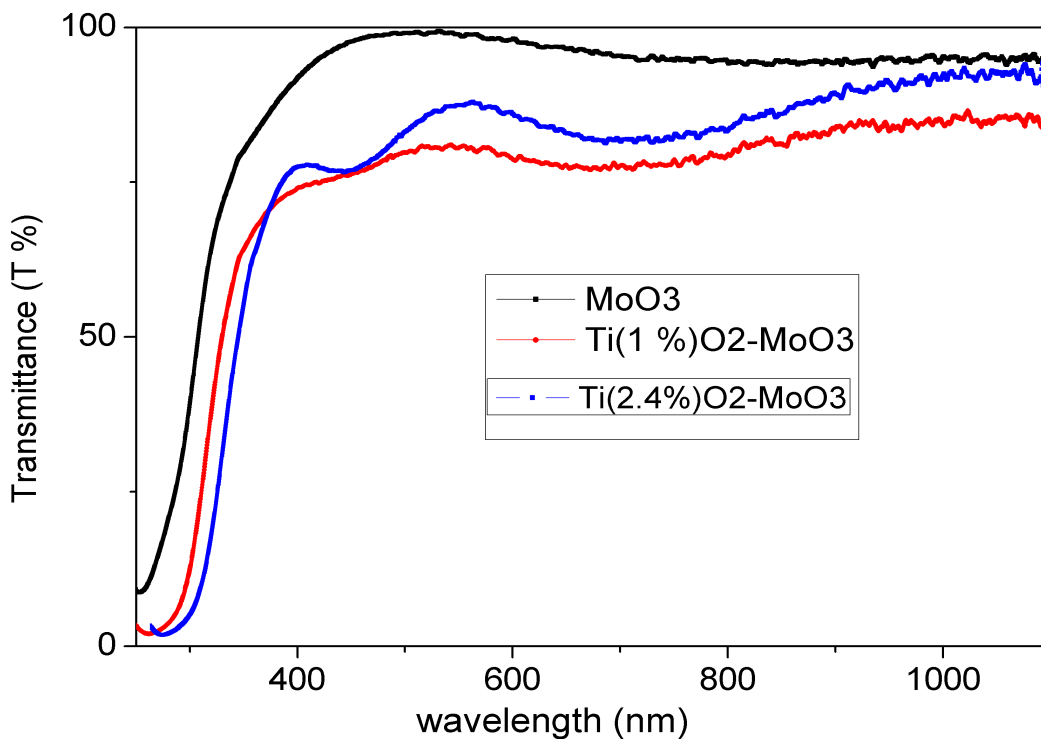


**Fig.11:** Optical transmittance spectra of MoO<sub>3</sub> and TiO<sub>2</sub>-MoO<sub>3</sub> thin films deposited at a sputtering pressure of 5 Pa and substrate temperature of 600 K.

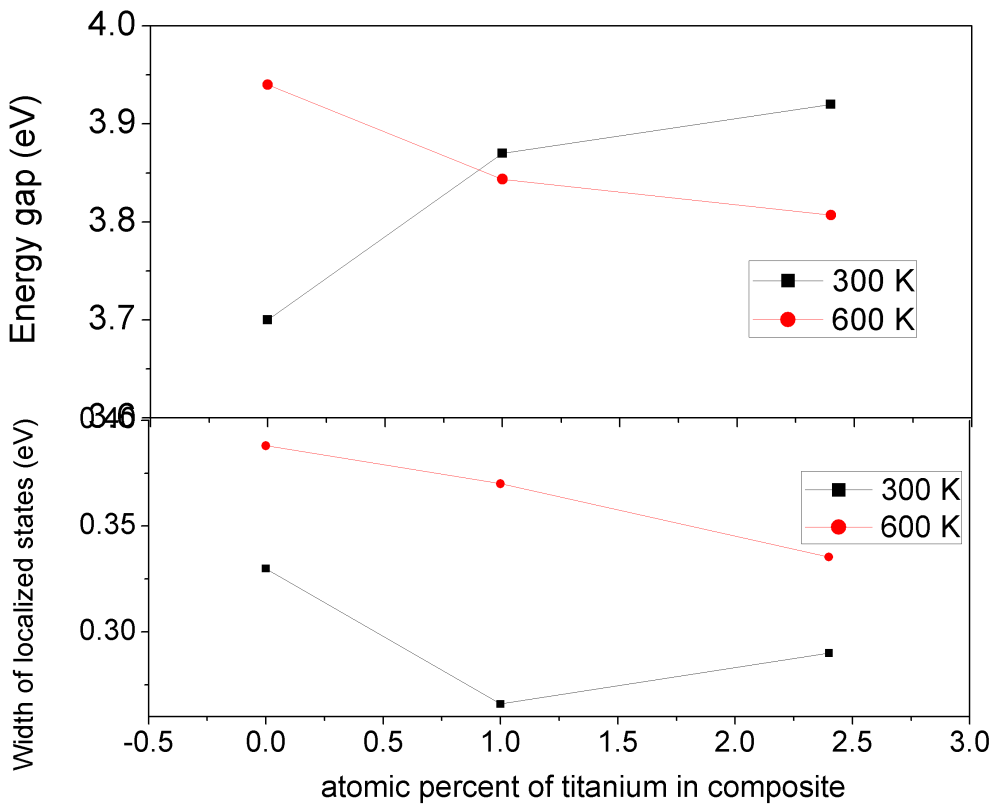


**Fig. 12:** variation of energy gap and width of localized states with Ti atomic percent in composite

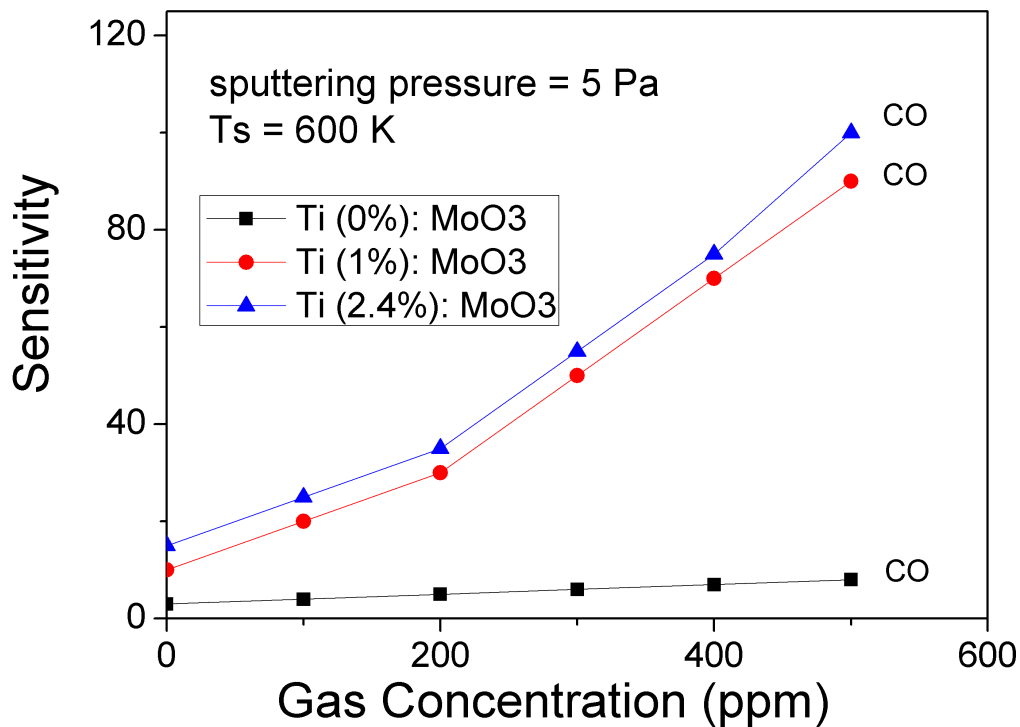


Fig. 13: Sensitivity of (TiO<sub>2</sub>):MoO<sub>3</sub> thin films for CO.

#### 4 Conclusions

MoO<sub>3</sub> and TiO<sub>2</sub>-MoO<sub>3</sub> thin films were deposited by d.c. magnetron sputtering. The binding energies of Mo and Oxygen shift towards lower energy with increasing polycrystallinity. The structural studies revealed that the composite films crystallized in orthorhombic phase were in compressive stress and this stress turned to tensile when films were crystallized in monoclinic phase. The optical results reveal that the tunability of the energy gap and transmittance to a required value. Moreover, the crystalline and Titanium-doped composite films were good candidates to detect toxic gas, CO.

The results revealed that the composite films of required stoichiometry, structure, surface morphology and good sensitivity to toxic gases can be obtained at optimized deposition conditions.

**Acknowledgments :** The authors are thankful to Dr. B. Tirumalarao, Scientific Officer E, from Raja Ramanna Centre for Advanced Technology (RRCAT), Indore, India for the UV-VIS measurements. The authors are thankful to the central instrumentation facility, Advanced Centre for Materials Science, IIT Kanpur, Kanpur, India for the XPS measurements. The authors are also thankful to the central instrumentation facility, IIT Guwahati, Guwahati, India for the FESEM measurement. The authors are also thankful to the technical cell of central equipment facility, S.N. Bose

National Centre for Basic Sciences, Kolkata, India for the GIXRD measurements.

#### Compliance with ethical standards

**Conflict of interest:** The authors have no conflict of interest.

#### References

- [1] O.M.Hussain, K. S. Rao, Characterization of activated reactive evaporated MoO<sub>3</sub> thin films for gas sensor applications, *Mater. Chem. and Phy* [http://doi:10.1016/S0254-0584\(03\)00101-9](http://doi:10.1016/S0254-0584(03)00101-9), **80**, 638 – 646, 2003.
- [2] G. F. Fine, L.M. Cavanagh, A. Afonja and R. Binions, *Metal Oxide Semi-Conductor Gas Sensors in Environmental Monitoring*, Sensors <https://doi.org/10.3390/s100605469>, **10**, 5469 - 5502, 2010.
- [3] T. Ivanova, K. A. Gesheva, A. Szekeres, Structure and optical properties of CVD molybdenum oxide films for electrochromic application, *J of Sol. Sta. Electro* <http://doi:10.1007/s10008-002-0274-7>, **7**, 21 – 24, 2002.
- [4] P.V. Kala, P. Mohan Babu, K. Srinivasarao, Optical, structural and electrochromic properties of nano crystalline MoO<sub>3</sub> thin films, *Mater. Res. India* <http://dx.doi.org/10.13005/msri/150105>, **15**, 41–47, 2018.

- [5] K. S. Rao, K.V. Madhruvi, S. Uthanna, O.M. Hussain and C. Julien, Photochromic properties of double layer CdS/MoO<sub>3</sub> Nano structured films, *Mater. Sci. & Engg. B* [https://doi.org/10.1016/S0921-5107\(03\)00078-3](https://doi.org/10.1016/S0921-5107(03)00078-3), **100** 79-86, 2003.
- [6] D. Li, M. Li, J. Pan, Y. Luo, H. Wu, Y. Zhang and G. Li, Hydrothermal Synthesis of Mo-Doped VO<sub>2</sub>/TiO<sub>2</sub> Composite Nanocrystals with Enhanced Thermochromic Performance, *Appl. Mater. and Interf.* <https://doi.org/10.1021/am500135d>, **6**, 6555 – 6561, 2014.
- [7] P. Jittiarporn, L. Sikong, K. Kooptarmond, W. Taweepreda, S. Stoenescu, S. Badilescu, V. Truong, Electrochromic properties of MoO<sub>3</sub>-WO<sub>3</sub> thin films prepared by a sol-gel method, in the presence of a triblock copolymer template, *Surf. and Coat. Tech.* <https://doi.org/10.1016/j.surfcoat.2017.08.012>, **327** 66-74, 2017.
- [8] C. M. Chohant, T. M. Westphal, R. D. C. Balboni, E. A. Moura, A. Gündel, W. H. Flores, A. Pawlicka, C. O. Avellaneda, Thin films of V<sub>2</sub>O<sub>5</sub>/MoO<sub>3</sub> and their applications in Electrochromism, *J. of Sol. Sta. Electrochem* <https://doi.org/10.1007/s10008-016-3491-1>, **21**, 1509 – 1515, 2017.
- [9] C. E. Patil, N. L. Tarwal, P. R. Jadhav, P. S. Shinde, H. P. Deshmukh, M. M. Karanjkar, A. V. Moholkar, M. G. Gang, J. H. Kim, P. S. Patil, Electrochromic performance of the mixed V<sub>2</sub>O<sub>5</sub>-WO<sub>3</sub> thin films synthesized by pulsed spray pyrolysis technique, *Curr. App. Phys.* <https://doi.org/10.1016/j.cap.2013.12.014>, **14** 389-395, 2014.
- [10] V. Sivaranjani, P. Deepa and P. Philominathan, Thin Films of TiO<sub>2</sub>-MoO<sub>3</sub> Binary Oxides Obtained by an Economically Viable and Simplified Spray Pyrolysis Technique for Gas Sensing Application, *Inter. J. of Thin Film Sci. and Tech.* <http://dx.doi.org/10.12785/ijtfst/040210>, **4**, 125 – 131, 2015.
- [11] X. Pang, H. Bian, M. Su, Y. Ren, J. Qi, H. Ma, D. Wu, L. Hu, B. Du, and Q. Wei, Photoelectrochemical Cytosensing of RAW264.7 Macrophage Cells Based on a TiO<sub>2</sub> Nanoneedles@MoO<sub>3</sub> Array, *Anal. Chem.* <https://doi.org/10.1021/acs.analchem.7b01038>, **89**, 7950-7957, 2017.
- [12] Y. Zhao, Q. Sun, J. Luo, H. Chen, W. Cai, X. Su, Hydrothermal fabrication of TiO<sub>2</sub>/MoO<sub>3</sub> nanocomposites with superior performance for water treatment, *Nano-Struc. & Nano-object* <https://doi.org/10.1016/j.nanoso.2017.12.003>, **13**, 13, 93-99, 2018.
- [13] Y. Li, K. Galatsis, W. Wlodarski, M. Ghantasala, S. Russo, J. Gorman, S. Santucci and M. Passacantando, Microstructure characterization of sol-gel prepared MoO<sub>3</sub>-TiO<sub>2</sub> thin films for oxygen gas sensors, *J. of Vac. Sci. & Tech. A : Vac. Surf. and Films* <https://doi.org/10.1116/1.1368676>, **19**, 904 – 909, 2011.
- [14] K. Galatsis, Y. X. Li, W. Wlodarski, E. Comini, G. Faglia, G. Sberveglieri, Semiconductor MoO<sub>3</sub>-TiO<sub>2</sub> thin film gas sensors, *Sens. and Act.* [https://doi.org/10.1016/S0925-4005\(01\)00737-7](https://doi.org/10.1016/S0925-4005(01)00737-7), **77**, 472 – 477, 2007.
- [15] T. Anwar, L. Wang, L. Jiaoyang, W. Chen, R. U. R. Sagar, L. Tongxiang, Lithium storage study on MoO<sub>3</sub>-grafted TiO<sub>2</sub> nanotube arrays, *App. Nano Sci.* <http://doi.org/10.1007/s13204-016-0526-y>, **6**, 1149 – 1157, 2016.
- [16] Mc Carron III E., J. Calabrese, The growth and single crystal structure of a high pressure phase of molybdenum trioxide: MoO<sub>3</sub>-II, *J. Sol. Sta. Chem.* [https://doi.org/10.1016/0022-4596\(91\)90064-O](https://doi.org/10.1016/0022-4596(91)90064-O), **91**, 121, 1991.
- [17] A. Q. Khan, S. Yuan, S. Niu, L. Zheng, W. Li and H. Zeng, Synthesis of molybdenum oxide-titanium dioxide nanocomposites with ultrashort laser ablation in water, *Opt. Expr.* <https://doi.org/10.1364/OE.25.00A539>, **25**, A539-A546, 2017.
- [18] N. E. Boboriko and D. I. Mychko *Inorganic Materials, Thermally stimulated transformations of sol-gel derived TiO<sub>2</sub>/MoO<sub>3</sub> composites*, *Inor. Mater.* <https://doi.org/10.1134/S0020168513080025>, **49** 795 – 801, 2013.
- [19] M. R. Ranade, S. H. Elder and A. Navrotsky, Energetic of Nanoarchitected TiO<sub>2</sub>-ZrO<sub>2</sub> and TiO<sub>2</sub>-MoO<sub>3</sub> Composite Materials, *Chem. Mater.* <http://doi.org/10.1021/cm010607u>, **14**, 1107 – 1114, 2002.
- [20] V. V. Atuchin, t. A. Gavrilova, G. Kostrovsky, L. d. Pokrovsky, I. B. Troitskaia, Morphology and structure of hexagonal MoO<sub>3</sub> nanorods, *Inor. Mater.* <https://doi.org/10.1134/S0020168508060149>, **44** 622-627, 2008.
- [21] N. Li, Y. Li, W. Li, S. Ji, P. Jin, One-Step Hydrothermal Synthesis of TiO<sub>2</sub>@MoO<sub>3</sub> Core-Shell Nanomaterial: Microstructure, Growth Mechanism, and Improved Photochromic Property, *J. of Phy. Chem. C* <http://doi.org/10.1021/acs.jpcc.5b10752>, **120**, 3341 – 3349, 2016.
- [22] J. Tauc, Optical properties and electronic structure of amorphous Ge and Si, *Journal of Mater. Res. Bull.* [https://doi.org/10.1016/0025-5408\(68\)90023-8](https://doi.org/10.1016/0025-5408(68)90023-8), **3**, 37 – 46, 1968.
- [23] S. Silvestri, E. T. Kubaski, T. Sequinel, S. A. Pianaro, J. A. Varela, S. M. Tebcheran, Optical Properties of the MoO<sub>3</sub>-TiO<sub>2</sub> Particulate System and Its Use as a Ceramic Pigment, *Part. Sci. and Tech.* <https://doi.org/10.1080/02726351.2013.773388>, **31** 466 – 473, 2013.
- [24] R. Swapana, M. C. Santhosh Kumar, Growth and characterization of molybdenum doped ZnO thin films by spray pyrolysis, *J. of Phy. and Chem. of Sol.*, **74**, (2013) 418-425, <https://doi.org/10.1016/j.jpcc.2012.11.003>.

- [25] K.Srinivasa Rao, B.Rajanikanth, P.K.Mukhopadhyay, Optical and IR studies on r.f. magnetron sputtered ultra-thin MoO<sub>3</sub> films, *Appl. Phy. - A: Mater. Sci. & Proc*<https://doi.org/10.1007/s00339-009-5132-3>, **96** 985-990, 2009.
- [26] S. Capene, R. Rella, P. Siciliano, L. Vosanelli, A comparison between V<sub>2</sub>O<sub>5</sub> and WO<sub>3</sub> thin films as sensitive elements for NO detection, *Thin Sol. Fil*[https://doi.org/10.1016/S0040-6090\(99\)00045-0](https://doi.org/10.1016/S0040-6090(99)00045-0), **350** 264, 1999.
- [27] C. F. Solzbacher, H. Steffecs, E. Obermeier, Gas-sensing characteristics of modified- MoO<sub>3</sub> thin films using Ti-overlayers for NH<sub>3</sub> gas sensors, *Sen. & Act. B:Chem*[https://doi.org/10.1016/S0925-4005\(99\)00506-7](https://doi.org/10.1016/S0925-4005(99)00506-7), **64**, 193 – 197, 2000.
- [28] O.M. Hussain, K.S. Rao, K.V. Madhuri, C.V. Ramana, B.S. Naidu, S. Pai, J. John and R. Pinto, Growth and characteristics of reactive pulsed laser deposited molybdenum trioxide thin films, *App. Phy. - A: Mater. Sci. & Proc.*<https://doi.org/10.1007/s003390100994>, **75**, 417- 422, 2002.